JEE Journal of Ecological Engineering

Journal of Ecological Engineering, 2026, 27(2), 401–411
https://doi.org/10.12911/22998993/211792
ISSN 2299–8993, License CC-BY 4.0

Received: 2025.09.30
Accepted: 2025.12.15
Published: 2026.01.15

Phosphorus adsorption mechanism from water by magnesium/calcium salt impregnated biochar

Phuong Van Nguyen[1]

[1] Institute of Environmental Science, Engineering and Management, Industrial University of Ho Chi Minh City, 12 Nguyen Van Bao Street, Hanh Thong Ward, Ho Chi Minh City 700000, Vietnam
E-mail: nguyenvanphuong@iuh.edu.vn

ABSTRACT

In recent years, excess phosphorus (P) discharged into surface water has caused environmental pollution. Therefore, the removal and recovery of phosphate are urgent needs that need to be developed. Biochar derived from macadamia shell impregnated with Ca (or Mg) was prepared to evaluate the adsorption and recovery of P from water. Batch adsorption experiments were performed to determine the optimal conditions for the adsorption process (initial pH, adsorbent dosage) and the adsorption mechanism of P on the material based on adsorption isotherm equilibrium, adsorption kinetics and FTIR spectral structure analysis. The results showed that Bio 300Mg and Bio 300Ca both exhibited high P adsorption and recovery capacities, with P adsorption capacities reaching 36 and 39 mg g^{-1}, and recovery efficiencies reaching 87.6 and 97.0%, respectively, at 10 g L^{-1} of Bio 300Ca and Bio 300Mg, initial P concentration of 400 mg L^{-1} and an initial pH of 4. The Freudlich isotherm model and pseudo-second-order kinetic model were used to explain the P adsorption mechanisms of the two materials. The main interaction mechanisms included: (1) electrostatic interactions, (2) hydrogen bonding, and (4) chemical co-precipitation and chemical precipitation. These results provide valuable insights for the development of efficient and environmentally friendly P-recovery biochar materials for reuse in agriculture.

Keywords: cation bridge, chemical adsorption, H-bonding, macadamia husk, P adsorption.

INTRODUCTION

Uncontrolled release of Phosphorus (P) into surface water must be managed, given its known role in causing eutrophication. This over-enrichment of water bodies severely disrupts the ecological balance and poses risks to human health, underscoring the need (Xu et al., 2022). Among the sources of P discharge, wastewater from livestock farming is of great concern (Choi et al., 2019; Xu et al., 2022). However, P is essential for plants, so this can be considered a source of P that should be recovered thoroughly. Effective recovery of P from wastewater not only alleviates the P deficiency crisis (non-renewable resource) but can also prevent pollution in surface waters (Xu et al., 2022). Biochar-based P adsorption is gaining more and more attention, as it is a cheap adsorbent from agricultural by-products and can be reused for agriculture (Choi et al., 2019).

From an adsorption perspective, the P anion's high hydration energy and the biochar's characteristic negatively charged surface create an electrostatic barrier. This strong repulsion is the primary factor limiting the adsorption of P from the aqueous phase (Choi et al., 2019; Xu et al., 2022). Therefore, research on biochar modification to improve P recovery efficiency from water is of great interest (Xu et al., 2022).

P in water exists mainly in the form of $H_2PO_4^-$, HPO_4^{2-}, which can interact strongly with positively charged ions in the order of priority $Na^+ < Mg^{2+} < Ca^{2+} < Al^{3+} < Fe^{3+}$. Metals coated on biochar form positively charged hydrates, which can attract P in water through electrostatic interactions and H bridges of hydrate molecules (Li et al., 2025). Furthermore, the study of Qiu et al showed that Ca-based biochar has a high ability to adsorb P in water, the product after the adsorption process slowly releases P into water, and has

great potential for application as fertilizer (Qiu et al., 2025). Using processes such as pyrolysis of biochar after it has been impregnated with metals (salt or hydroxide form) is complex and energy intensive (Deng et al., 2021; Qiu et al., 2025). Biochar coated with heavy metals has the risk of secondary pollution. Therefore, the current study considers the process of impregnating biochar with Mg (or Ca) salts at ambient temperature, drying, and then using it as a P adsorbent. Ca and Mg are also essential secondary nutrients for plants.

A better understanding of the mechanism of P adsorption onto the material can help predict its potential for future fertilizer applications. Adsorption equilibrium and kinetic studies provide useful information on surface properties, adsorption mechanisms, and interactions between the adsorbent and the adsorbate. Common adsorption isotherm equations, such as Langmuir, Freundlich, and first-order and second-order kinetic models, are often used to clarify these mechanisms (Lima et al., 2015). In addition, FTIR spectral analysis supports clarifying the interaction forces of cations (Ca, Mg) coated on the biochar surface during P adsorption. However, studies on the adsorption mechanism of P in water based on biochar derived from macadamia shell impregnated with Ca, Mg salts are still lacking information.

According to the Dak Nong Department of Agriculture, the macadamia growing area in the region is expected to increase from about 6.506 hectares (2022–2025 period) to 10,923 hectares in 2030, and reach 13,105 hectares in 2050. With a yield of 1.5 tons of nuts/ha, the amount of waste shells accounts for 3/4 of the total output, which is an abundant source of raw materials for biochar production. According to previous research, biochar derived from macadamia husk pyrolyzed at 300 °C has a higher P adsorption capacity in water than biochar pyrolyzed at higher temperatures (450 and 600 °C) and also requires less energy (Van Phuong, 2025).

The objectives of the study include (i) determining the parameters affecting P adsorption (pH, dosage); (ii) P adsorption mechanisms based on adsorption equilibrium and kinetic studies. Furthermore, changes in surface chemistry of Mg (or Ca) salt-impregnated biochar were also examined, including pH, pHpzc, and surface functional groups (before and after P adsorption) based on FTIR analysis. The study clarifies the P adsorption mechanism on modified biochar as a theoretical basis for the application of the recovered product as a slow-release fertilizer.

MATERIALS AND METHODS

Chemicals

All chemicals, including: $(NH_4)_6Mo_7O_{24}\cdot 4H_2O$, NaH_2PO_4, NaOH, $K_2Cr_2O_7$, H_2SO_4, $SnCl_2$, $MgCl_2$ $6H_2O$, $CaCl_2$ $6H_2O$, were of analytical grade and sourced from Merck and China. Standard solution 1000 mgP/L prepared from NaH_2PO_4.

Experimental setup

Preparation of adsorbent material: biochar impregnated with $CaCl_2$ (or $MgCl_2$)

The process is carried out through 2 stages: (1) biochar preparation, (2) biochar impregnated with Ca, Mg salts.

1. Biochar preparation – macadamia husks are pyrolyzed at 300 °C, heating rate 10 °C/min, retention time 2 h, cooled, ground through a 1 mm sieve, (named Bio 300). The surface chemical properties of Bio 300 are presented in detail in a previous study (Van Phuong, 2025).
2. Weigh accurately 20.0 g Bio 300, impregnate with 400 mL of 1M $CaCl_2$ solution (named Bio 300Ca), and in case with 1M $MgCl_2$ (named Bio 300Mg), shake continuously for 24 hours using a GFL 3015 (Germany) circular shaker at 300 rpm. Then, the samples were filtered with 90 mm Whatman filter paper (without water washing), dried at 105 °C to constant weight (about 4 hours), ground through a 1mm sieve, and stored in glass jars with lids (Arbelaez Breton et al., 2021; Choi et al., 2019). Some of the surface properties of Bio 300Mg (or Bio 300Ca) were determined, including pH, pH point of zero charge (pHpzc) (Tu, 2016), identification of surface functional groups was achieved via FTIR spectral analysis (JASCO FT/IR-4700 type A) within the 350−4000 cm^{-1} range.

Survey of influencing factors: initial pH, adsorbent dosage

The experiment was simulated based on previous studies (Deng et al., 2021; Van Phuong, 2025). Specifically, accurately weigh 0.3 g of Bio 300Ca (or Bio 300Mg) sample with 30 mL

of 200 mgP/L solution in a 50 mL centrifuge tube with predetermined initial pH values and not adjusted during the experiment. The mixture was then shaken on a GFL 3015 circular shaker at 350 rpm for 24 hours to ensure P adsorption reached equilibrium (based on preliminary studies). The solid and liquid phases were separated by centrifuging the suspension at 5000 rpm for 5 minutes (DLAB DM 0636 centrifuge), followed by filtering the supernatant through a 0.22 µm filter. The P content in the final solution was quantified via absorption spectroscopy using a GENESYS 10S UV-VIS, USA. All adsorption experiments were performed in triplicate. The predetermined initial pH parameters were 2, 4, 6, 8, and 10 (adjusted with 0.1 mol L^{-1} HCl and NaOH solutions).

The experiment to determine the adsorbent dosage was conducted similarly to the experiment to investigate the initial pH effect. The adsorption conditions included an initial P concentration of 200 mg L^{-1}, the pH was selected from the previous experiment, and the dosage of Bio 300Mg (or Bio 300Ca) was changed respectively to 3.3, 10.0, 16.7, 23.3, and 33.3 g L^{-1}.

Evaluation parameters include P adsorption capacity (mg g^{-1}) and recovery efficiency (%). For P recovery as a by-product for agricultural use, efficiency will be considered first.

Survey of P adsorption equilibrium

The adsorption equilibrium survey of P onto Bio 300Ca (or Bio 300Mg) was simulated according to previous studies (Arbelaez Breton et al., 2021; Choi et al., 2019; Van Phuong, 2025). The experiment was carried out in a 50 mL polypropylene centrifuge tube by shaking 0.3 g of biochar with 30 mL of a solution containing 200 mg P L^{-1} under the conditions: initial pH and dosage of the material used were selected from the previous experiment, and with a series of initial P concentrations (0, 25, 50, 100, 150, 200 and 400 mg P L^{-1}) for 24 h. The subsequent steps were carried out as described previously. Langmuir and Freundlich models were used to examine the fit of the adsorption isotherms to the experimental data.

Survey of adsorption kinetics of phosphorus

The experiment was carried out in a 50 mL polypropylene centrifuge tube by shaking 0.3 g of Bio 300Ca (or Bio 300Mg) with 30 mL of a solution containing 200 mgP L^{-1} at the pH selected in the previous experiment. The remaining steps were like those mentioned above. After different time intervals (20, 40, 80, 160, and 320 min), the samples were collected, centrifuged, filtered, and analyzed for P (Arbelaez Breton et al., 2021; Choi et al., 2019).

Data analysis

Calculation of adsorption equilibrium

P adsorption capacity from water, mg g^{-1}, Equation 1:

$$q_i = \frac{(C_0 - C_i).V}{m} \quad (1)$$

$$\mathrm{H\%} = \frac{(C_0 - C_i).100}{C_i} \quad (2)$$

where: C_0 (mg L^{-1}): initial P concentration, Ci (mg L^{-1}): P concentration adsorbed at equilibrium time, V (L): volume of P solution, m (g): mass of material sample, qi (mg g^{-1}): P adsorption capacity of sample i at equilibrium time, H%: recovery efficiency, Equation 2.

Langmuir isotherm equation, Equation 3:

$$\frac{1}{q_i} = \frac{1}{K_L q_0}\frac{1}{C_i} + \frac{1}{q_0} \quad (3)$$

where: K_L is Langmuir adsorption constant (L mg^{-1}).

Freundlich isotherm equation, Equation 4:

$$q = y/m = K_F C^{\frac{1}{n_F}} \quad (4)$$

where: n_F – Freundlich isotherm constant, represents the P adsorption intensity,
K_F – Freundlich adsorption isotherm constant, represents the adsorption capacity.

Calculation of adsorption kinetics

To study the adsorption mechanism, pseudo-first-order and pseudo-second-order adsorption kinetic models are often used to analyze and model the kinetic adsorption data (Sun and Wang, 2016).

Pseudo-first-order adsorption kinetic equation, Equation 5:

$$Ln(q_e - q_t) = -k_1 t + Lnq_e \quad (5)$$

Pseudo-second-order adsorption kinetics equation, Equation 6:

$$\frac{1}{q_t} = \frac{1}{t}\frac{1}{k_2 q_e^2} + \frac{1}{q_e} \quad (6)$$

where: q_e – adsorption capacity P at equilibrium time (mg g^{-1}); q_t – adsorption capacity P at time t; k_1 (1 min^{-1}) and k_2 (g mg^{-1} min^{-1}) are pseudo-first-order and pseudo-second-order adsorption kinetic constants; t – adsorption time (min).

Data processing

All data were compiled and statistically analyzed using Excel software. To ensure the reliability of the results, all experiments and analyses were conducted in triplicate. One-way analysis of variance (ANOVA) was used to compare the mean values of independent groups to determine whether there was a statistically significant difference between their mean values.

RESULTS AND DISCUSSION

Some surface chemical properties of materials

Some properties of Bio 300Ca and Bio 300Mg have been presented in detail in Table 1. The results showed that the pH of the two material samples in the study decreased compared to the pH of Bio 300. Specifically, 6.65 and 5.36 respectively, for Bio 300Ca and Bio 300Mg compared to Bio 300 in the previous study (Van Phuong, 2025). This may be due to the hydrolysis of Mg and Ca salts on the surface of biochar, releasing protons. Similarly, the pHpzc of the two material samples also decreased, but the decrease was not statistically significant, 6.15 and 5.86, respectively. When the environmental pH is lower than pHpzc, the material surface is positively charged. During the adsorption process, anions will be absorbed onto the material surface, enhancing the efficiency of the adsorption process.

Figure 1 shows that the spectral peaks in the range 2934–3447 cm^{-1} are assigned to the H-bond stretching vibrations of the O-H groups of water molecules and of the hydroxyl functional groups. The peak 3728 cm^{-1} is assigned to the O-H vibrations of hydrate molecules in $Ca(OH)_2$ or $Mg(OH)_2$ (Nandhini et al., 2019). The peaks at 1583 cm^{-1} are the stretching vibration of the aromatic group C=C, and the peaks at 1450 cm^{-1} correspond to the vibration of the carboxyl group (-COOH). A medium intensity peak of the CaO (or MgO) stretching vibration appeared at 422 cm^{-1} for Bio 300Mg and Bio 300Ca (Nandhini et al., 2019). Furthermore, the strong adsorption peaks (1450, 1583, and 2934 cm^{-1}) of Bio 300Mg, Bio 300Ca show that there are more functional groups on the modified biochar than on the original Bio 300 (Figure 1) (Deng et al., 2021).

Effect of initial solution pH

The results of the initial pH effect on the P adsorption capacity of Bio 300Mg and Bio 300Ca under the condition of material dosage of 10.0 g L^{-1}, concentration of 200 Pmg $L^{-1,}$ were presented in Figure 2A. With Bio 300Mg, the P adsorption capacity increased significantly when the pH increased from 3 to 4. Then, it decreased insignificantly when the pH continued to increase, specifically, the P adsorption capacity was 15.0, 17.1, 12.9, 13.2, and 13.0 mgP g^{-1} corresponding to the initial pH of 3, 4, 6, 8, and 10, respectively. With Bio 300Ca, at pH 3 and 4, the P adsorption capacity was high at 17.5 and 18.4 mgP g^{-1}, respectively. Then it decreased significantly at pH 6 and pH 8; the decrease was not significant at 16.0 and 16.2, respectively. At pH 10, the adsorption capacity decreased significantly to 14.8 mgP g^{-1} (Figure 2A). When the initial pH increased to 4, this pH was still <pHpzc of Bio 300Mg and Bio 300Ca (6.2 and 5.9), so the biochar surface was positively charged, favorable for the adsorption of P anions ($H_2PO_4^-$, HPO_4^{2-}). When the initial pH increased >6, exceeding the pHpzc of the two material samples (Table 1), the material surface became negatively charged, leading to an unfavorable adsorption process (Deng et al., 2021; Xu et al., 2022). In addition, OH^- ions in alkaline solution compete with P molecules for adsorption sites, resulting in reduced P adsorption capacity (Deng et al., 2021; Yang et al., 2016). The adsorption process of P onto Bio 300Ca was higher than that of Bio 300Mg at all initial pH levels (Figure 2A). In addition to electrostatic interactions, Bio 300Ca may also have a chemical precipitation reaction between P anion and CaO or $Ca(OH)_2$ on the material surface (Xu et al., 2022).

With the P recovery efficiency from water (Figure 2B), it was shown that pH 4 gave the highest P recovery efficiency of 92.0% and 85.6% for Bio 300Ca and Bio 300Mg, respectively. At higher

Table 1. Some surface chemical properties of biochar-based material samples

Materials	pH	pHpzc
Bio 300	7.09[c]	6.35[a]
SD	0.11	0.14
Bio 300Ca	6.65[b]	6.15[a]
SD	0.12	0,36
Bio 300Mg	5.36[a]	5.86[a]
SD	0.30	0.30

Note: SD – standard deviation. Different letters a, b, c in the same column indicate statistically significant differences.

pH, the recovery efficiency was lower, which was explained similarly to the effect of initial pH on P adsorption capacity. The results showed that pH 4 was chosen for the next experiments.

Effect of adsorbent dosage

The results of the investigation of the influence of Bio 300Mg and Bio 300Ca dosages on P adsorption under conditions such as pH 4, P content of 200 mg L^{-1}, are presented in Figure 3A. The results showed that the P adsorption capacity decreased by 47.5, 17.4, 8.9, 6.7, and 4.0 mg g^{-1} with Bio 300Mg, and with Bio 300Ca, the adsorption capacity was 47.1, 18.4, 9.1, 5.9, and 4.5 mg g^{-1}, respectively, corresponding to the material dosages of 3.3, 10.0, 16.7, 23.3, and 33.3 g L^{-1}. This can be explained by the fact that when the adsorbent dosage increased, but the P content in the solution was limited, leading to a decrease in P adsorption capacity (Deng et al., 2021)

When the dosage of Bio 300Mg and Bio 300Ca increased from 3.3 to 10.0 g L^{-1}, the P recovery efficiency increased insignificantly, from 79.2 to 86.8%, and from 78.5 to 92.0%, respectively, Figure 3B. This was mainly due to the small number of adsorption sites compared to the amount of P in the water (Deng et al., 2021). When the dosage of the material continued to increase, the P recovery efficiency decreased; however, the decrease was not statistically significant (Figure 3B). This case is explained by the phenomenon of aggregation of the material particles, thereby strongly reducing the active sites and leading to a decline in the recovery efficiency of Phosphorus (P) (Van Phuong, 2025).

In the experiment, when increasing the dosage of 2 materials used, the P adsorption capacity decreased. However, the P recovery efficiency increased the most at the dosage of 10g L^{-1}. Prioritizing the recovery parameters, the material dosage of 10g L^{-1} was selected.

P adsorption equilibrium

Figure 4A shows that the P adsorption capacity on Bio 300Mg and Bio 300Ca increased significantly under experimental conditions (initial pH 4, adsorbent dosage 10 g L^{-1}). Specifically, with Bio 300Mg, the P adsorption capacity was 0.0, 0.7, 2.2, 6.9, 11.6, 16.0 and 35.3 mg g^{-1}, respectively, with Bio 300Ca, it was 0.0, 1.9, 4.3, 9.0, 13.6, 18.8 and 38.6 mg g^{-1}, respectively, with initial P concentrations of 0, 25, 50, 100, 150, 200 and 400 mg L^{-1}. This can be explained by the fact that increasing the initial P concentration increases the chance of contact between P and the adsorbent,

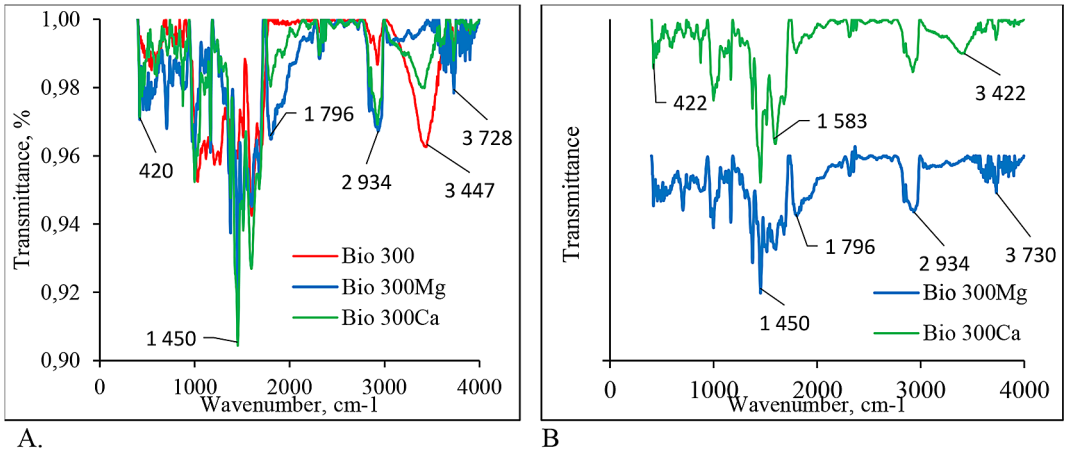

Figure 1. FTIR spectra of macadamia shell biochar-based materials: (A) compared with the original Bio 300 spectrum, (B) compared with the Bio 300Mg and Bio 300Ca spectra

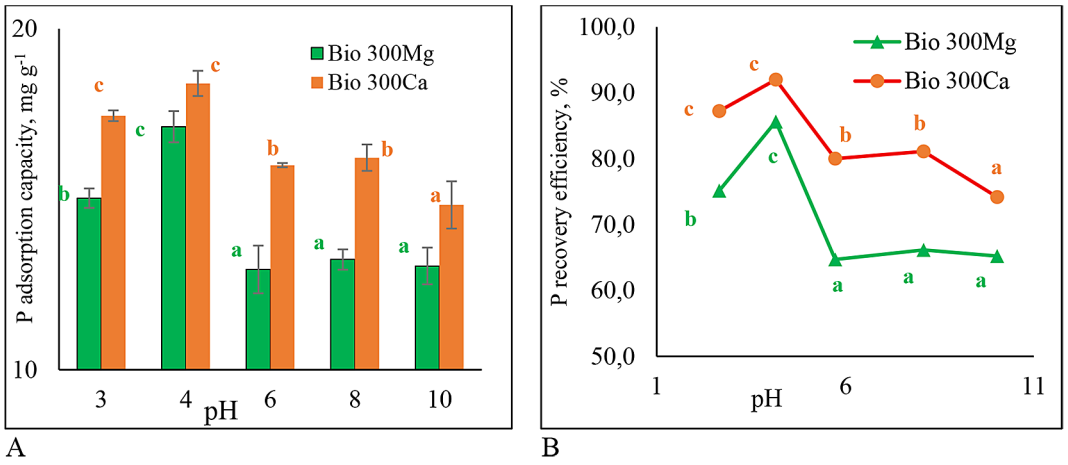

Figure 2. Effect of initial pH on adsorption capacity of P (A) and recovery efficiency of P (B) in water (Different letters a, b, c on the same-colored graphs indicate significant differences)

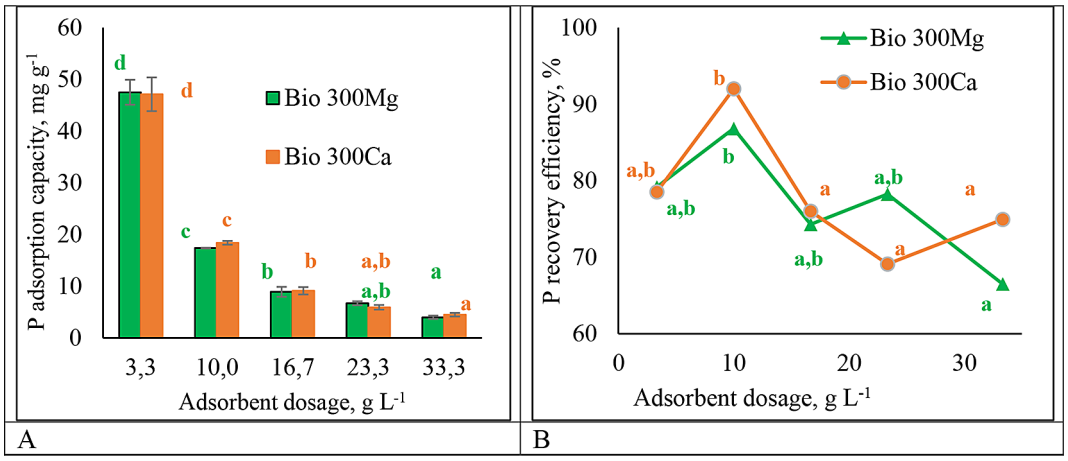

Figure 3. Effect of adsorbent dosage on P adsorption capacity (A) and P recovery efficiency (B) (different letters a, b, c, d of the same color on the graphs indicate significant differences)

increasing the adsorption capacity (Khalil et al., 2018). One-way ANOVA analysis results showed that the P adsorption process of the two materials increased, with no sign of adsorption saturation under experimental conditions when increasing the initial P concentration. This can be explained in terms of a constant distribution isotherm, where new adsorption sites appear immediately after the solute is adsorbed onto the material surface from the solution (Tan, 2011; Van Phuong, 2025). In the case study, these could be newly formed hydrogen bonds via P−OH...O=P bridges, hydrated cation bridges, electrostatic and van Der Waals forces, surface coprecipitation, and chemical precipitation (Tan, 2011; Tomczak et al., 2019).

P recovery efficiency in water (Figure 4B) showed that Bio 300Ca had a significantly higher P recovery efficiency than Bio 300Mg at each initial P concentration. Specifically, with Bio 300Ca, the efficiencies were 0, 77, 87, 90, 90, 94, and 97%, respectively, with Bio 300Mg being 0, 15, 39, 66, 75, 79, and 88%, respectively, with initial P concentrations of 0, 25, 50, 100, 150, 200 and 400 mg L^{-1}. One-way ANOVA analysis confirmed that the P recovery process in water by Bio 300Mg or Bio 300Ca took place in 2 stages, (i) the stage of reaching saturation recovery efficiency corresponding to a certain initial P concentration and (ii) the stage of maintaining recovery efficiency (changes with no statistical significance) if the initial P concentration continued to increase (Figure 4B). Specifically, in stage 1, with Bio 300Mg, the recovery efficiency was 200 mgP $L^{-1,}$ and the recovery efficiency was 78.5%, with Bio 300Ca at 150 mgP $L^{-1,}$ and the efficiency reached 90.0%. Then, when continuing to increase the P concentration, the change in

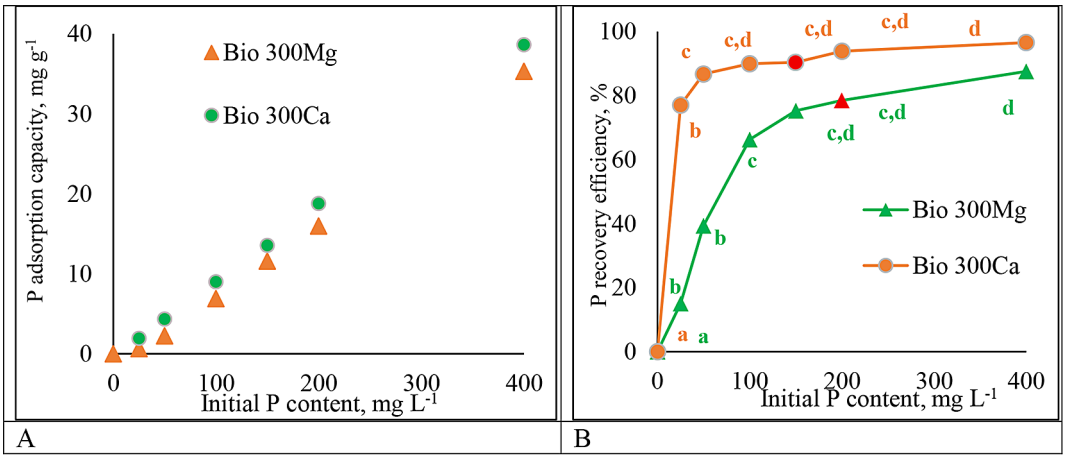

Figure 4. Initial P concentration on P adsorption capacity (A) and P recovery efficiency (B) in water (Different letters a, b, c, d of the same color on the graphs indicate significant differences)

P recovery efficiency from water changed with no statistical significance (Figure 4B).

The calculation results (Table 2) showed that the correlation (R^2) of the Langmuir model was tight with R^2 of 0.96 and 0.99 for Bio 300Mg and Bio 300Ca, respectively. However, the maximum adsorption capacity (q_0) had a value (negative value) very different from the experimental adsorption capacity value, q(Ex), Table 2, so the Langmuir model was not suitable to explain the P adsorption equilibrium from water. For the Freudlich model, R^2 was 0.95 and 0.98 for Bio 300Mg and Bio 300Ca, respectively, and this model was completely suitable to explain the P adsorption mechanism in water for the two materials. K_F was 0.054 and 0.006, respectively, and $1/n_F$ was 1.75 and 3.33, respectively. The value of $1/\eta_F$ represents the adsorption intensity on a heterogeneous surface (Feng et al., 2021). This confirms that the adsorption surface is not uniform, and the adsorption process is chemical adsorption (Lima et al., 2015). The results obtained differ from some studies that suggested that the Langmuir model was more suitable, which may be due to the different preparation procedures, with the pyrolysis regime performed last (Feng et al., 2021)

Under experimental conditions with pH 4, initial P content of 400 mg L^{-1}, the P adsorption capacity of Bio 300Mg and Bio 300Ca samples was 36 and 39 mg g^{-1} (Table 2). The research results were different from the previously reported results (Table 3) (Arbelaez Breton et al., 2021). Specifically, Mg^{2+} impregnated biochars including Poplar chips, Holm oak, Greenhouse paprika waste, have adsorption capacities of 89, 65, 65 mg g^{-1} respectively. While Ca^{2+} impregnated raw biochars gave lower results in the study (13.6 mg g^{-1}). This may be due to the influence of many factors such as pyrolysis conditions, impregnation solution type and adsorption conditions. Therefore, experimental research for each specific material cannot be ignored.

Adsorption kinetics of P

The adsorption process of P onto two experimental materials with different contact times, Figure 5A and 5B, showed that the adsorption

Table 2. P adsorption equilibrium parameters

Models	Materials	Parameters		R^2	q(Ex)
		q_0 (mg g^{-1})	K_L		
Langmuir	Bio 300Mg	-8.79	0.96	0.96	36
	Bio 300Ca	-2.80	0.99	0.99	39
Freundlich		$1/n_F$	K_F		
	Bio 300Mg	1.75	5.44E-02	0.95	
	Bio 300Ca	3.33	5.73E-03	0.98	

Note: q(Ex): experimental adsorption capacity of P.

Table 3. P adsorption capacity of some biochar samples impregnated with metal salts

Models	Materials	q_e (mg g^{-1})	Kinetic constant		q(Ex)	R^2
Pseudo-first-order kinetic	Bio 300Mg	2.53	k_1	0.001	18.5	0.59
	Bio 300Ca	3.67		0.001	18.1	0.86
Pseudo-second-order kinetic	Bio 300Mg	18.28	k_2	0.018	18.5	0.90
	Bio 300Ca	17.47		0.016	18.1	0.90

Note: Source – Arbelaez Breton et al. (2021).

kinetics occurred in three main stages – fast (P diffusion onto the material surface), slow (diffusion inside the material), and equilibrium (completion of diffusion into smaller pores) (Lima et al., 2015). With Bio 300Mg, the first stage is the fastest: after 20 minutes, the P adsorption capacity reaches 16.0 mg L^{-1}, efficiency 80% (significant increase), the slowing stage: after the next 20 minutes with the adsorption capacity of 16.7 mg L^{-1}, the efficiency increases by 2.1% (insignificant increase), the equilibrium stage: after 80 minutes, the capacity only increases by 4% and is considered saturated. Similar to Bio 300Ca, the adsorption capacity of P was 14.9, 16.1, and 16.6 mg g^{-1}, and recovery efficiency was 74, 81, and 83% corresponding to adsorption times of 20, 40, and 80 minutes. This phenomenon can be explained by the fact that in the initial stage, the large number of active sites on the material surface leads to a rapid increase in adsorption capacity. After this period, the number of unadsorbed sites decreases, the adsorption capacity increases slowly and remains stable, so the efficiency increases insignificantly (Lima et al., 2015; Van Phuong, 2025)

The results of calculating the kinetic parameters in the study (Table 4) showed that, with the pseudo-first-order kinetic model, the correlation R^2 was 0.59 and 0.86, respectively. However, the calculated qe values were completely inconsistent with the experimental values, q(Ex). Specifically, the calculated qe for Bio 300Mg and Bio 300Ca were 2.53 and 3.67 mg g^{-1}, while the experimental values, q(Ex), ranged from 18.5 to 18.1 mg g^{-1}. Therefore, the pseudo-first-order kinetic model was not suitable to explain the kinetics of P adsorption onto the two materials in the study.

With the pseudo-second-order kinetic model (Table 4), it was shown that R^2 = 0.90 for both Bio 300Mg and Bio 300Ca, and the calculated qe results were also consistent with the experimental results, q(Ex). Therefore, the pseudo-second-order kinetic model used to explain the kinetics of P adsorption process is appropriate. This observation also means that the control of the kinetic process has the contribution of the chemical adsorption process. The removal mechanism through adsorption of the two types of materials is related to electrostatic interactions, the effect of hydrogen bonding and co-precipitation (Li et al., 2025). Similar conclusion was also found in

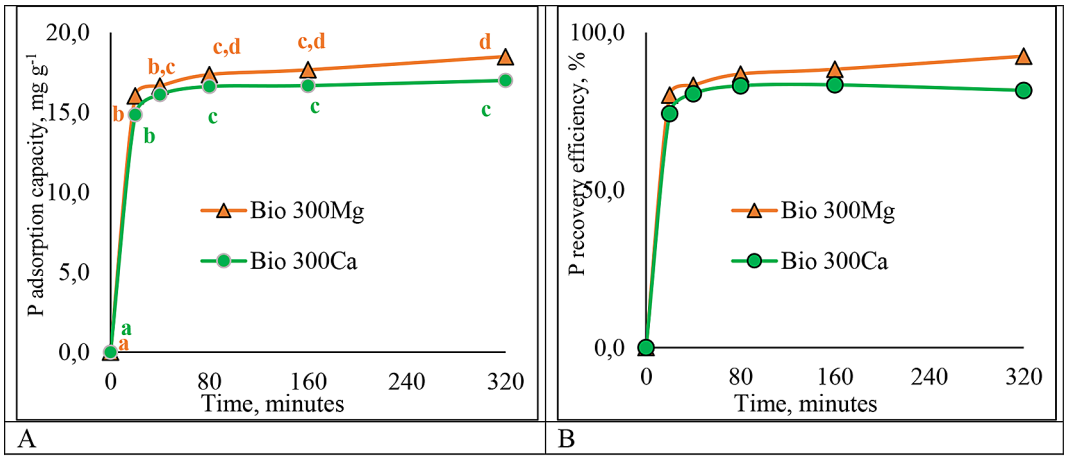

Figure 5. Changes in P adsorption capacity (A) and P recovery efficiency (B) over time (Different letters a, b, c of the same color on the graphs indicate significant differences)

Table 4. Adsorption kinetic parameters

Models	Materials	q_e (mg g^{-1})	Kinetic constant		q(Ex)	R^2
Pseudo-first-order kinetic	Bio 300Mg	2.53	k_1	0.001	18.5	0.59
	Bio 300Ca	3.67		0.001	18.1	0.86
Pseudo-second-order kinetic	Bio 300Mg	18.28	k_2	0.018	18.5	0.90
	Bio 300Ca	17.47		0.016	18.1	0.90

the study of Qiu et al, suggesting that the P adsorption mechanism of Ca-based biochar mainly included surface precipitation, ion exchange, and electrostatic attraction (Qiu et al., 2025). The results are also consistent with the previously determined Freundlich adsorption isotherm model, which assumes that chemical adsorption controls the process (Table 2).

Figure 6A shows that the peaks of Bio 300Mg have vibrational bands at 2932 and 3439 cm−1, which are attributed to the broadening and stronger -OH stretching vibrational band after P adsorption, indicating the strong involvement of hydrogen bonding through the -OH bridge of hydrate molecules. In addition, Bio 300Mg has a broad stretching vibrational band from 999 cm^{-1} to 1454 $cm^{-1,}$ which is attributed to the presence of PO_4^{3-} group (Berzina-Cimdina and Borodajenko, 2012), and H-O-H bending of hydroxyl functional groups (Deng et al., 2021). Most of the spectral peaks of Bio 300Mg at these positions became stronger after P adsorption, which might be due to the formation of intramolecular and intermolecular hydrogen bonds during P adsorption (Deng et al., 2021). Therefore, hydrogen bonding bridges played an important role in the adsorption of P by Bio 300Mg. Similar results were also found in the study of Hu et al., suggesting that hydrated cations (Ca, Mg) act as bridges to connect anions through hydrogen bonding of hydrated cation bridges (Hu et al., 2023).

The FTIR spectrum of Bio 300Ca sample after P adsorption also has similar functional groups as Bio 300Mg (Figure 6A). However, the -OH stretching vibration band decreased sharply or disappeared after P adsorption (peaks 2932 and 3439 cm^{-1}) and was replaced by a new absorption band assigned to the bending vibration of P−O at 1582 cm^{-1} (Fang et al., 2022). The obvious change of spectrum between Bio 300Ca before and after adsorption can be attributed to the interaction between -OH groups in hydrate molecules decreased sharply compared to Bio 300Mg (Figure 6B), indicating the existence of not many water molecules in the product after adsorption or in other words, there was the formation of calcium phosphate chemical precipitation (Feng et al., 2021). Similar results and explanations were also found in the studies of Feng et al and Xu et al, suggesting that the adsorption mechanism was based on ligand exchange between Ca^{2+} and phosphate near the surface of Ca-coated biochar, followed by surface precipitation (Deng et al., 2021; Xu et al., 2022).

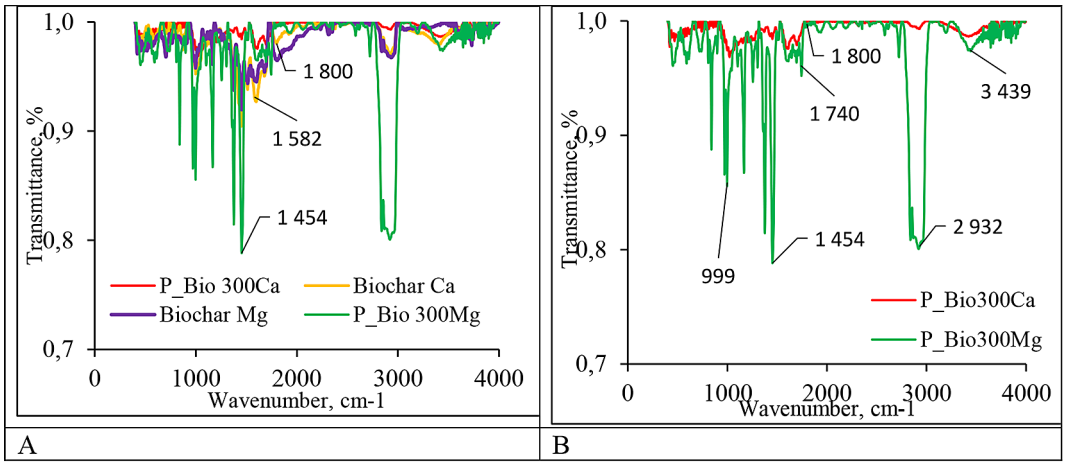

Figure 6. FTIR spectra of Bio 300-based materials: (A) comparison of spectra before and after P adsorption, (B) comparison of Bio 300Mg and Bio 300Ca spectra after P adsorption

CONCLUSIONS

Two types of adsorbent materials (Bio 300Mg, and Bio 300Ca) were prepared from 300 °C pyrolysis biochar derived from macadamia husks impregnated with 1M $MgCl_2$ and 1M $CaCl_2$ solutions. Some surface properties, adsorption conditions, and optimal P recovery efficiency were also determined. The results showed that Bio 300Mg and Bio 300Ca both exhibited high P adsorption and recovery capacity, with P adsorption capacity reaching 36 and 39 mg g^{-1}, and recovery efficiency reaching 87.6 and 97.0% corresponding to an initial P concentration of 400 mg L, and an initial pH of 4. The results showed that Bio 300Ca had higher phosphate adsorption and recovery capacity than Bio 300Mg. The Freudlich isotherm model and pseudo-second-order kinetic model were suitable to explain the P adsorption mechanism of the two materials. The primary mechanisms governing this process included electrostatic interaction, hydrogen bonding, and chemical co-precipitation/precipitation. These findings offer valuable insights for developing highly efficient and environmentally sustainable biochar-based materials to recover phosphorus (P) waste from wastewater.

Acknowledgements

This study was conducted with the support of students majoring in Environmental Engineering, Course 15. We also express our deep gratitude to the reviewers for their in-depth comments, which contributed significantly to improving the manuscript.

REFERENCES

1. Arbelaez Breton, L., Mahdi, Z., Pratt, C., El Hanandeh, A. (2021). Modification of hardwood derived biochar to improve phosphorus adsorption. *Environments*, *8*(5), 41.
2. Berzina-Cimdina, L., Borodajenko, N. (2012). Research of calcium phosphates using Fourier transform infrared spectroscopy. *Infrared spectroscopy-materials science, engineering and technology*, *12*(7), 251–263.
3. Choi, Y.-K., Jang, H. M., Kan, E., Wallace, A. R., Sun, W. (2019). Adsorption of phosphate in water on a novel calcium hydroxide-coated dairy manure-derived biochar. *Environmental Engineering Research*, *24*(3), 434–442.
4. Deng, Y., Li, M., Zhang, Z., Liu, Q., Jiang, K., Tian, J., Zhang, Y., Ni, F. (2021). Comparative study on characteristics and mechanism of phosphate adsorption on Mg/Al modified biochar. *Journal of Environmental Chemical Engineering*, *9*(2), 105079.
5. Fang, Y., Ali, A., Gao, Y., Zhao, P., Li, R., Li, X., Liu, J., Luo, Y., Peng, Y., Wang, H. (2022). Preparation and characterization of MgO hybrid biochar and its mechanism for high efficient recovery of phosphorus from aqueous media. *Biochar*, *4*(1), 40.
6. Feng, D., Lü, J., Guo, S., Li, J. (2021). Biochar enhanced the degradation of organic pollutants through a Fenton process using trace aqueous iron. *Journal of Environmental Chemical Engineering*, *9*(1), 104677.
7. Feng, Y., Zhao, D., Qiu, S., He, Q., Luo, Y., Zhang, K., Shen, S., Wang, F. (2021). Adsorption of phosphate in aqueous phase by biochar prepared from sheep manure and modified by oyster shells. *ACS omega*, *6*(48), 33046–33056.
8. Hu, Y., Wang, H., Lu, X., Sun, L., Wu, Y., Fang, J., Dai, C. (2023). Study on the effective methods for breaking hydrated cation bridges between crude oil and quartz. *Journal of Molecular Liquids*, *385*, 122271.
9. Khalil, A., Sergeevich, N., Borisova, V. (2018). Removal of ammonium from fish farms by biochar obtained from rice straw: Isotherm and kinetic studies for ammonium adsorption. *Adsorption Science & Technology*, *36*(5–6), 1294–1309.
10. Li, Y., Zhu, Y., Liu, J., Fan, W., Cao, Y., Huo, Y., Wei, J. (2025). Review of modified biochar for removing humic acid from water: analysis of structure-activity relationship. *Biochar*, *7*(1), 1.
11. Lima, É. C., Adebayo, M. A., Machado, F. M. (2015). Kinetic and equilibrium models of adsorption. In *Carbon nanomaterials as adsorbents for environmental and biological applications* 33–69. Springer.
12. Nandhini, D., Subashchandrabose, S., Ramesh, P., Radheep, D. M., Sakthipandi, K. (2019). Synthesis, characterization and computation of potassium doped calcium hydroxide nanoparticle and nanotubes. *International Journal of Mechanical and Production Engineering Research and Development*, *9*, 441–448.
13. Qiu, X., Zheng, J., Yan, X., Davronbek, B., Garcia-Mina, J. M., Zhou, H., Zhao, Q., Chai, L., Lin, Z., Zhang, L. (2025). Preparation of calcium-based phosphate adsorbent and mineral-rich humic acid fertilizer from biomass ash and bamboo by hydrothermal-pyrolysis: Performance and mechanism. *Environmental Research*, *264*, 120318.
14. Sun, H., Wang, X. (2016). NH4+ adsorption and adsorption kinetics by sediments in a drinking water reservoir. *Archives of Environmental Protection*, *42*(4). https://doi.org/10.1515/aep-2016-0039

15. Tan, K. H. (2011). *Principles of soil chemistry, Fourth Edition*. Taylor and Francis Group, LLC.
16. Tomczak, W., Boyer, P., Krimissa, M., Radakovitch, O. (2019). Kd distributions in freshwater systems as a function of material type, mass-volume ratio, dissolved organic carbon and pH. *Applied Geochemistry*, *105*, 68–77.
17. Tu, T. (2016). Physical and chemical characterization of biochar derived from rice husk. *Hue Univ. J. Sci*, *120*, 233–247.
18. Van Phuong, N. (2025). Mechanism and behavior of phosphorus adsorption from water by biochar forms derived from macadamia husks. *Nature Environment & Pollution Technology*, *24*(1).
19. Xu, Y., Liao, H., Zhang, J., Lu, H., He, X., Zhang, Y., Wu, Z., Wang, H., Lu, M. (2022). A novel Ca-modified Biochar for efficient recovery of phosphorus from aqueous solution and its application as a phosphorus biofertilizer. *Nanomaterials*, *12*(16), 2755.
20. Yang, G., Wu, L., Xian, Q., Shen, F., Wu, J., Zhang, Y. (2016). Removal of congo red and methylene blue from aqueous solutions by vermicompost-derived biochars. *PLoS ONE*, *11*(5), 1–19.